Occurrence of Rotation Domains in Heteroepitaxy

Marius Grundmann,* Tammo Böntgen, and Michael Lorenz
Institut für Experimentelle Physik II, Universität Leipzig, D-04103 Leipzig, Germany
(Received 9 June 2010; published 28 September 2010)

Heteroepitaxy can involve materials with a misfit of crystal structure. Rotation domains in the epilayer are a fundamental consequence. We derive a general expression for their (minimum) number which is determined by the mismatch of the rotational symmetries of the substrate and epilayer. In the case of a mismatch of rotational symmetry, the number of rotation domains of material A on material B is different from that of B on A. A larger number of rotation domains can occur due to domain structure or nearly fulfilled additional symmetries of the substrate surface.

DOI: 10.1103/PhysRevLett.105.146102 PACS numbers: 68.55.−a, 68.47.Fg, 77.84.−s

Heteroepitaxy is a prerequisite step for the fabrication of the active structures of many modern solid-state electronic and photonic devices. Heteroepitaxy is also used for the growth of such structures on substrates. Typical examples of epitaxy on heterosubstrates are GaN on Al_2O_3 and GaAs on Si.

Generally, the substrate and epilayer can be quite dissimilar and belong to different crystal structures and have different lattice parameters. The mismatch of *translational* symmetry (lattice constants) leads to specific defects (dislocations). This phenomenon has been investigated extensively, and the concept of domain epitaxy explains and allows for a variety of advanced matching conditions by defined in-plane rotation of lattices [1–4]. Here, we treat the effect of the mismatch of *rotational* symmetry, leading to rotation domains as a consequential defect. Rotation domains can occur already in bulk materials; see, e.g., [5]. Here we restrict ourselves to materials that are single phase and single domain in bulk form. The substrate surface and epilayer shall have C_n and C_m symmetry, respectively, with regard to the surface normal, possible values being $n, m \in \{1, 2, 3, 4, 6\}$ [6].

Rotation domains in the epilayer are domains with the same crystallographic direction along the growth direction but different in-plane azimuthal orientation. They are a *fundamental* consequence of the mismatch ($n \neq m$) of rotational symmetry across the heterointerface. The occurrence and orientation of rotation domains has been reported in the literature for several specific material combinations. A unified picture and generalized theoretical treatment is missing; even in the extensive review of Pond [4] on the crystallography of domain formation and dislocations in layered systems, only the case of zinc blende on a diamond structure (GaAs on Si or Ge) has been treated. Using group theory, we derive here a general formula for the (minimum) number of rotational domains that applies to all possible cases of rotational mismatch in heteroepitaxy.

The presence of rotation domains necessarily introduces large-angle (tilt) grain boundaries into the epilayer. From a practical standpoint, detrimental consequences may result for the epilayer properties (such as larger surface roughness, inhomogeneous strain and impurity distribution, reduced carrier diffusion length, mobility and lifetime, larger concentration of deep levels, or lower efficiency of radiative recombination), depending on the distribution of domain sizes. Subsequently, device properties (such as breakdown voltage, leakage current, noise, cutoff frequency, or quantum efficiency) are adversely effected.

Hexagonal GaN(00.1) on twofold symmetric AlAs(001) exhibits only a single domain [7] ($N_{RD} = 1$). Hexagonal ZnO(00.1) on Si(001) leads to two domains in the epilayer, rotated 90° (or due to the 60° symmetry rotated apparently 30°) against each other [8]. A notable case with $N_{RD} = 3$ is fourfold symmetric (tetragonal) BTO(001) on hexagonal ZnO(00.1) [Figs. 1(a) and 1(c)] [9]. The domains are rotated 30° against each other. The inverted case of ZnO (00.1) on BTO(001) yields a different number of rotation domains [Figs. 1(b) and 1(d)] $N_{RD} = 2$. They are rotated 90° against each other [10]. The orthorhombic $BiFeO_3$(001) with C_1 symmetry on Si(001) leads to $N_{RD} = 4$ domains, rotated 90° against each other [11].

All such cases can be explained with the mismatch of rotational symmetry at the interface, resulting in

$$N_{RD} = \mathrm{lcm}(n, m)/m. \quad (1)$$

The substrate is invariant under cyclic group C_n with rotation angles $\phi_i = 2\pi i/n$, the epilayer crystal under cyclic group C_m with $\phi_j = 2\pi j/m$, i and j being integers. The epilayer orientation is thus invariant for rotation angles $\phi_i + \phi_j = 2\pi(i/n + j/m) = 2\pi k/\mathrm{lcm}(n, m) = \psi_k$, with $\mathrm{lcm}(n, m)$ being the least common multiple of n and m, and k being an integer. Bézout's theorem yields that, for each k, values i and j exist [12]. Thus the rotations with angles ψ_k form a cyclic group C' of order $\mathrm{lcm}(n, m)$. One possible rotation domain is given by the subgroup C_m of C'. The number of equivalent rotation domains N_{RD} is given by the number of equivalent classes (or orbits) of order m (index of C_m in C') yielding (1) with Lagrange's theorem [13].

For (n, m), there are a total of 25 possible combinations (Table I): 12 such combinations yield a single domain, 5

 © 2010 The American Physical Society

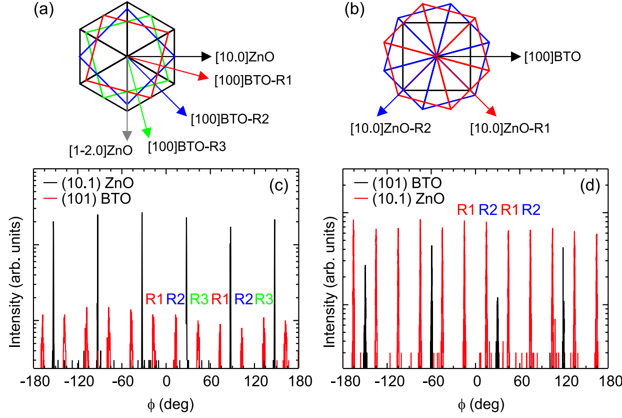

FIG. 1 (color online). (c) High-resolution x-ray diffraction ϕ scan of 250 nm $BaTiO_3(001)$ thin film (BTO) on ZnO(00.1) (550 nm ZnO thin film on a-plane Al_2O_3). ZnO shows the sixfold symmetry of its (10.1) planes ($\Psi = 61.61°$, $2\Theta = 36.254°$). The $BaTiO_3$ (101) ($\Psi = 45.28°$, $2\Theta = 31.483°$) exhibits 12 30°-spaced peaks indicating that the C_4-symmetric (tetragonal) layer aligns in-plane within three rotational domains as shown schematically in (a). (d) High-resolution x-ray diffraction ϕ scan of 800 nm ZnO(00.1) thin film on an 800 nm BTO (001) layer on a STO(001) substrate. BTO exhibits the fourfold symmetry of its (101) planes. The ZnO (10.1) planes exhibit 12 30°-spaced peaks indicating that the hexagonal layer aligns in-plane with two rotation domains as shown schematically in (b).

combinations yield $N_{RD} = 2$ rotation domains, 5 combinations result in three, and 2 cases in four rotation domains. Six domains occur for one combination. If $n = m$, the number of rotation domains is 1. For all other combinations ($n \neq m$), the inverse material sequence yields a different number of rotational domains. The approach here is simplified with respect to the mirror symmetries of the substrate; in a forthcoming publication, we discuss all 150 cases arising from the ten 2D point symmetries.

The case $n = 4$, $m = 6$ is particularly interesting, e.g., cubic (or tetragonal) BTO(001) and hexagonal ZnO(00.1). It is a situation where neither the A/B nor the inverted B/A ($n = 6$, $m = 4$) material sequence exhibits a single domain. Recent advances in epitaxial ferroelectric gates on semiconductor channels for transparent and programmable transistors [10,14] require the growth of these materials for the active structure. Depending on whether a top gate or bottom gate device design is chosen, the epitaxial heterostructure is BTO on ZnO or ZnO on BTO, respectively.

TABLE I. Number of rotational domains N_{RD} according to Eq. (1); n and m denote the C_n and C_m rotational symmetries of the substrate and epilayer, respectively.

$n\backslash m$	1	2	3	4	6
1	1	1	1	1	1
2	2	1	2	1	1
3	3	3	1	3	1
4	4	2	4	1	2
6	6	3	2	3	1

A case of $n = 6$ and $m = 4$, leading to $N_{RD} = 3$, could also be a bixbyite (bcc cubic) or a rocksalt (001) epilayer on a hexagonal substrate. However, only [111]-oriented growth of such epilayers has been reported, e.g., for $In_2O_3(111)$ on InN(0001) [15] and MgO(111) on c-plane ZnO(00.1) [16]. Another case resulting in $N_{RD} = 3$ is $n = 6$ and $m = 2$. This could be realized by a zinc blende (001) layer on a hexagonal substrate. Such a combination also often grows with the epilayer in [111] orientation, e.g., AlN(111) on $Al_2O_3(00.1)$ [17]. The results in Ref. [18] about $In_2O_3(001)$ and InN(001) on c-plane Al_2O_3 are, however, inconclusive with regard to rotation domains. For twofold symmetric orthorhombic β-$FeSi_2(101)$ [or (110)] on Si(111) indeed three rotation domains are observed [19]. A case of $n = 6$ and $m = 1$, leading to $N_{RD} = 6$, could be orthorhombic U_3O_8 on c-plane Al_2O_3. In Ref. [20], indeed a sixfold symmetry of the U_3O_8 epilayer is found; however, it is attributed rather to a new, epitaxially induced hexagonal symmetry than to the presence of six rotation domains of orthorhombic material.

An extreme case poses an amorphous substrate; here the epilayer can take any azimuthal orientation. If it grows in columnar grains, the azimuthal orientation from grain to grain largely fluctuates [21], giving it effectively C_∞ symmetry.

As can be seen from the above examples and Table II, Eq. (1) describes the number of rotation domains correctly for many epitaxial systems. We have not found an experimental example in our work and the literature where N_{RD} is smaller than given by Eq. (1). It can, however, be *larger* than that given by (1) due to (i) domain structure or (ii) additional "nearly fulfilled" symmetries of the substrate surface. In the following, we discuss a few prominent examples.

A well-known case of crystal structure misfit is zinc blende on diamond with the formation of antiphase boundaries [4], e.g., for InP(001)/Si(001) [28]. The [001] direction in bulk Si and InP has fourfold symmetry. However, a Si(001) surface with monolayer ($a_0/2$) steps exhibits two C_2 domains (on the terraces), while the zinc blende (001) surface has uniformly twofold symmetry (C_2). The antiphase domains in the zinc blende material are inversion domains and can be considered as two rotation domains ($N_{RD} = 2$) with their [110] or $[1\bar{1}0]$ direction aligned with the Si [110] direction, respectively. A similar case arises for hexagonal ZnO(00.1) on Si(001). The two C_2 domains on the substrate lead to two ZnO domains not related by inversion, rotated 90° against each other [8].

Hexagonal ZnO(00.1) on $Al_2O_3(00.1)$ often shows the expected single domain growth [3,45]. However, this system has also been observed to exhibit two rotation domains [31,32] with a relative azimuth of 30°. The additional second domain nucleates only under certain growth conditions (oxygen pretreatment) that generate monolayer steps and a mix of Al- and O-terminated surface. This situation is conceptually similar to the Si(001) surface with monolayer steps offering two C_2 domains, rotated 90° against each other. Even the occurrence of three rotation domains (30° and 21.8°) has been observed [47]

TABLE II. Various epitaxial systems with match ($n = m$) and mismatch ($n \neq m$) of rotational symmetry. N_{RD} denotes the number of rotation domains expected from Eq. (1). The number d of domains present on the substrate surface is given as a number in round brackets ($\times d$) in the first column. Column "Exp." hosts the number of experimentally observed domains.

n	m	Substrate	Epilayer	N_{RD}	Exp.	Ref.
1	1	Al_2O_3(01.2)	ZnO(11.0)	1	1	[22,23]
1	1	Al_2O_3(01.2)	SW-CNT	1	1	[24]
1	2	Al_2O_3(01.2)	InN(001)	1	1	[25]
1	3	Al_2O_3(01.2)	CeO_2(111)	1	2[b]	[26]
1	4	Al_2O_3(01.2)	CeO_2(001)	1	1	[26]
2	1	Al_2O_3(11.0)	SW-CNT	2	2	[24]
2	2	GaAs(001)	AlAs(001)	1	1	[27]
2	2	Si(001)BL	InP(001)	1	1	[28]
2 ($\times$ 2)	2	Si(001)ML	InP(001)	1	2[a]	[28]
2	3	GaAs(001)	MgO(111)	2	2	[29]
2	4	GaAs(001)	MgO(001)	1	1	[30]
2	6	AlAs(001)	GaN(00.1)	1	1	[7]
2	6	Al_2O_3(11.0)	ZnO(00.1)	1	1	[31,32]
2 ($\times$ 2)	6	Si(001)	ZnO(00.1)	1	2[a]	[8]
3	1	Si(111)	SW-CNT	3	6[b]	[33]
3	2	Si(111)	$FeSi_2$(101)	3	3	[19]
3	3	Si(111)	Ge(111)	1	1	[34]
3	4	Si(111)	$FeSi_2$(001)	3	6[b]	[35]
3	6	Si(111)	ZnO(00.1)	1	1	[36]
4	1	STO(001)	BFO(001)	4	4	[11]
4	1	MgO(001)	SW-CNT	4	4	[37]
4	2	NaCl(001)	ZnO($2\bar{1}$.0)	2	2	[38]
4	2	STO(001)	ZnO(11.0)	2	4[b]	[39]
4	3	MgO(001)	CuCl(111)	4	4	[40]
4	4	NaCl(001)	AgCl(100)	1	1	[41]
4	6	BTO(001)	ZnO(00.1)	2	2	[42], Fig. 1
6	1	Al_2O_3(00.1)	U_3O_8(001)	6	6[c]	[20]
6	2	ZnO(00.1)	$LiGaO_2$(001)	3	3	[43]
6	3	ZnO(00.1)	MgO(111)	2	2	[16]
6	4	ZnO(00.1)	BTO(001)	3	3	Fig. 1
6	6	ZnO(00.1)	GaN(00.1)	1	1	[44]
6	6	Al_2O_3(00.1)	ZnO(00.1)	1	1	[45,46]
6 ($\times$ 2)	6	Al_2O_3(00.1)	ZnO(00.1)	1	2[a]	[31,32]
6 ($\times$ 3)	6	Al_2O_3(00.1)	ZnO(00.1)	1	3[a]	[47]
∞	6	SiO_2	ZnO(00.1)	∞	∞	[8,21]

[a]Indicates larger number of domains than (1) due to domains on the substrate surface.
[b]Indicates additional domains due to nearly fulfilled symmetries. BTO denotes $BaTiO_3$; STO, $SrTiO_3$; BFO, $BiFeO_4$; SW-CNT, single-wall carbon nanotube; Si(001)ML denotes a Si(001) surface with monolayer steps (height of $a_0/2$), and Si(001)BL denotes a Si(001) surface with bilayer steps (height of a_0). Al_2O_3(11.0) is the a plane; Al_2O_3(01.2) is the r plane.
[c]Indicates unsure assignment.

for hydrogen pretreatment. Ga pretreatment [47] or nitridation of the sapphire substrate [48] eliminates such additional domains.

In Ref. [35], three rotation domains are observed as expected for β-$FeSi_2$(100) on Si(111), aligning the epilayer [010] with Si$\langle\bar{1}10\rangle$. Under certain growth conditions six rotation domains, separated by 15°, are observed, adding alignment of the epilayer [011] with Si$\langle\bar{1}01\rangle$ [35]. These two in-plane alignments seem to have similarly favorable energetics.

ZnO(11.0) [22], InN(001) [25], and Si(100) [49] all grow as single domain films on C_1-symmetric Al_2O_3(01.2) (r plane). CeO_2(111) on Al_2O_3(01.2) is also expected to grow as a single domain but is observed to exhibit two domains with the relative azimuth of 85.7° [26]. This occurs because the r plane of sapphire is "pseudocubic" and offers another similar, almost perpendicular direction for nucleation, aligning the [110] direction of CeO_2 with [$\bar{2}$2.1] and [$\bar{2}\,\bar{4}$.1] of Al_2O_3. For the growth of C_2-symmetric ZnO(11.0) on C_4-symmetric NaCl(001), two domains occur as expected [38]. On $SrTiO_3$(001), a second set of two domains appears, rotated 4° from the first set due to two nearly coincident site lattices [39].

We are grateful to H. Hochmuth, who has fabricated the BTO/ZnO and ZnO/BTO samples. This work has been supported by the Deutsche Forschungsgemeinschaft in

the framework of SFB 762 (Functionality of Oxidic Interfaces). T. B. is additionally supported by Leipzig School of Natural Sciences "Building with Molecules and Nano-objects (BuildMoNa)" (GS 185/1).

*grundmann@physik.uni-leipzig.de

[1] F. Grey and J. Bohr, Europhys. Lett. **18**, 717 (1992).
[2] J. Narayan and B. C. Larson, J. Appl. Phys. **93**, 278 (2003).
[3] G. F. Kuznetsov and S. A. Aitkhozhin, Crystallogr. Rep. **47**, 514 (2002).
[4] R. C. Pond, Crit. Rev. Solid State Mater. Sci. **15**, 441 (1989).
[5] D. S. Zhou and T. E. Mitchell, Philos. Mag. A **72**, 1131 (1995).
[6] The rotational symmetry of the arrangement of substrate surface atoms (2D lattice) can be different from that of its normal axis in bulk material. For example, the [001] direction in zinc blende is a fourfold axis, while the (001) surface has twofold symmetry. Possible bond rearrangement in surface reconstructions is broken up during the formation of covalent bonds in heteroepitaxy; thus, surface symmetry modified due to surface reconstructions is not considered important here.
[7] M. Funato, T. Ishido, A. Hamaguchi, S. Fujita, and S. Fujita, Appl. Phys. Lett. **77**, 244 (2000).
[8] Z. W. Liu, C. W. Sun, J. F. Gu, and Q. Y. Zhang, Appl. Phys. Lett. **88**, 251911 (2006).
[9] Our BTO/ZnO and ZnO/BTO heterostructures have been grown by pulsed laser deposition. Further details about the growth method can be found in Ref. [10].
[10] M. Brandt, H. Frenzel, H. Hochmuth, M. Lorenz, M. Grundmann, and J. Schubert, J. Vac. Sci. Technol. B **27**, 1789 (2009).
[11] F. Zavaliche, S. Y. Yang, T. Zhao, Y. H. Chu, M. P. Cruz, C. B. Eom, and R. Ramesh, Phase Transit. **79**, 991 (2006).
[12] The diophantine equation $1 = ia + jb$ with nonzero $a = 1\ \mathrm{cm}(n, m)/n$ and $b = 1\ \mathrm{cm}(n, m)/m$ has a solution since the greatest common denominator $\gcd(a, b) = 1$ [Bézout's identity; see, e.g., G. A. Jones and J. M. Jones, *Elementary Number Theory* (Springer-Verlag, Berlin, 1998), pp. 7–11]. Thus also $k = ia + jb$ has a solution.
[13] Lagrange's theorem; see, e.g., R. L. Roth, Math. Mag. **74**, 99 (2001).
[14] V. M. Voora *et al.*, Phys. Rev. B **81**, 195307 (2010).
[15] Ch. Y. Wang *et al.*, Phys. Status Solidi C **5**, 1627 (2008).
[16] H. Saitoh, Y. Okada, and S. Ohshio, J. Mater. Sci. **37**, 4597 (2002).
[17] K. Sumitani, R. Ohtani, T. Yoshida, Y. Nakagawa, S. Mohri, and T. Yoshitake, Jpn. J. Appl. Phys. **49**, 020212 (2010).
[18] F. M. Morales, J. G. Lozano, R. García, V. Lebedev, Ch. Y. Wang, V. Cimalla, O. Ambacher, and D. González, Phys. Status Solidi C **5**, 514 (2008).
[19] N. Cherief, C. D'Anterroches, R. C. Cinti, T. A. Nguyen Tan, and J. Derrien, Appl. Phys. Lett. **55**, 1671 (1989).
[20] A. K. Burrell, T. M. McCleskey, P. Shukla, H. Wang, T. Durakiewicz, D. P. Moore, C. G. Olson, J. J. Joyce, and Q. Jia, Adv. Mater. **19**, 3559 (2007).
[21] S. Heitsch *et al.*, Thin Solid Films **496**, 234 (2006).
[22] S. Liang, C. R. Gorla, N. Emanetoglu, Y. Liu, W. E. Mayo, and Y. Lu, J. Electron. Mater. **27**, L72 (1998).
[23] S. K. Han, S. K. Hong, J. W. Lee, J. Y. Lee, J. H. Song, Y. S. Nam, S. K. Chang, T. Minegishi, and T. Yao, J. Cryst. Growth **309**, 121 (2007).
[24] N. Ishigami, H. Ago, T. Nishi, K. Ikeda, M. Tsuji, T. Ikuta, and K. Takahashi, J. Am. Chem. Soc. **130**, 17 264 (2008).
[25] V. Cimalla, J. Pezoldt, G. Ecke, R. Kosiba, O. Ambacher, L. Spieß, G. Teichert, H. Lu, and W. J. Schaff, Appl. Phys. Lett. **83**, 3468 (2003).
[26] M. Sunder and P. D. Moran, J. Electron. Mater. **38**, 1931 (2009).
[27] C. Weisbuch, Semicond. Semimet. **24**, 1 (1987).
[28] M. Grundmann, A. Krost, and D. Bimberg, Appl. Phys. Lett. **58**, 284 (1991).
[29] E. J. Tarsa, M. De Graef, D. R. Clarke, A. C. Gossard, and J. S. Speck, J. Appl. Phys. **73**, 3276 (1993).
[30] K. Nashimoto, D. K. Fork, and T. H. Geballe, Appl. Phys. Lett. **60**, 1199 (1992).
[31] P. Fons, K. Iwata, A. Yamada, K. Matsubara, S. Niki, K. Nakahara, T. Tanabe, and H. Takasu, Appl. Phys. Lett. **77**, 1801 (2000).
[32] K. Nakahara, H. Takasu, P. Fons, K. Iwata, A. Yamada, K. Matsubara, R. Hunger, and S. Niki, J. Cryst. Growth **227–228**, 923 (2001).
[33] M. Su, B. Maynor, A. Buldum, J. P. Lu, and J. Liu, J. Phys. Chem. B **104**, 6505 (2000).
[34] V. Alberts, J. H. Neethling, and J. S. Vermaak, J. Mater. Sci. Mater. Electron. **3**, 240 (1992).
[35] A. Rizzi, B. N. E. Rösen, D. Freundt, Ch. Dieker, H. Lüth, and D. Gerthsen, Phys. Rev. B **51**, 17 780 (1995).
[36] Y. W. Zhang, X. M. Li, W. D. Yu, X. D. Gao, Y. F. Gu, C. Yang, J. L. Zhao, X. W. Sun, S. T. Tan, J. F. Kong, and W. Z. Shen, J. Phys. D **41**, 205105 (2008).
[37] M. Maret, K. Hostache, M.-C. Schouler, B. Marcus, F. Roussel-Dherbey, M. Albrecht, and P. Gadelle, Carbon **45**, 180 (2007).
[38] J.-H. Shen, S.-W. Yeh, H.-L. Huang, and D. Gan, Scr. Mater. **61**, 785 (2009).
[39] X. H. Wei, Y. R. Li, J. Zhu, W. Huang, Y. Zhang, W. B. Luo, and H. Ji, Appl. Phys. Lett. **90**, 151918 (2007).
[40] A. Yanase, Y. Segawa, M. Mihara, W. M. Tong, and R. S. Williams, Surf. Sci. Lett. **278**, L105 (1992).
[41] H. Haefke, R. Mattheis, and M. Krohn, Thin Solid Films **195**, 225 (1991).
[42] X. H. Wei, Y. R. Li, W. J. Jie, J. L. Tang, H. Z. Zeng, W. Huang, Y. Zhang, and J. Zhu, J. Phys. D **40**, 7502 (2007).
[43] I. Ohkubo *et al.*, J. Appl. Phys. **92**, 5587 (2002).
[44] A. Kobayashi, H. Fujioka, J. Ohta, and M. Oshima, Jpn. J. Appl. Phys. **43**, L53 (2004).
[45] N. Ashkenov *et al.*, J. Appl. Phys. **93**, 126 (2003).
[46] M. Grundmann, *The Physics of Semiconductors, An Introduction including Devices and Nanophysics* (Springer, Heidelberg, 2006), p. 282.
[47] X. L. Du, M. Murakami, H. Iwaki, and A. Yoshikawa, Phys. Status Solidi A **192**, 183 (2002).
[48] M. Ying, X. Du, Z. Mei, Z. Zeng, H. Zheng, Y. Wang, J. Jia, Z. Zhang, and Q. Xue, J. Phys. D **37**, 3058 (2004).
[49] H. M. Manasevit and W. J. Simpson, J. Appl. Phys. **35**, 1349 (1964).